CONTRAST AGENT DETECTION BASED ON AUTOREGRESSIVE SPECTRAL ESTIMATION

I. Dydenko[†,*]**, N. Rognin**[†]**, F. Jamal**[‡]**, D. Friboulet**[†]**, C. Cachard**[†]

[†]CREATIS, INSA, Bâtiment Blaise Pascal, 69621 Villeurbanne Cedex, France
[‡]Hôpital Cardiologique, Explorations Fonctionnelles Cardio-Vasculaires, Lyon, France
[*]Email: dydenko@creatis.insa-lyon.fr

Abstract

In this paper, we present a spectral autoregressive contrast detection method dedicated to the identification of ultrasound contrast agent in radiofrequency (RF) images, acquired with standard scanning devices used in echocardiography. This method is based on second-order autoregressive modeling of the RF signal, and it relies on the presence of the second harmonic component. It is dedicated to processing single RF frames. Numerical simulations, as well as in vitro investigations show that the proposed approach enables to correctly detect the contrast agent, in particular at low concentrations of the agent. It is also shown that an associated technique of discontinuity adaptive smoothing enables to obtain a binary map of contrast agent-perfused areas.

Introduction

Coronary artery disease remains a major cause of mortality in industrial countries, emphasizing the important role of early identification and prevention. Myocardial blood flow and flow reserve can be predicted based on ultrasound contrast agent (USCA) imaging, and in this context, reliable identification of tissues perfused with USCA in echographic images is of major medical interest.

In the present work, we describe a method for detection of USCA in single frames of radiofrequence (RF) images. Contrarily to several recently proposed methods [9], [12], it does not require special acquisition protocols or instrumentation. Our approach relies on the identification of the second harmonic component in the backscattered signal, resulting from the non-linear behaviour of USCA. It is based on autoregressive (AR) modeling of the spectrum.

In related work, multi-pulse methods were described to detect the non-linear effects of USCA by consecutive transmitting two or more different pulses. Let us cite pulse inversion [9], power modulation (Philips Medical Systems) or pulse inversion Doppler [12]. Single-pulse methods rely on the identification of the second harmonic [4], higher order harmonic [3] or subharmonic [6] components of the agent's acoustic response. In the same framework, [1] proposed a method called differential contrast echography, and recently, new emission protocols such as chirped excitation were proposed to enhance the harmonic component in USCA response

and suppress it in the tissue one [2].

Methodology

The contrast agent has a non-linear response in the range of frequencies used in cardiac echography and as a result, the spectrum of the RF signal acquired from USCA shows the presence of the second harmonic component. In this work, we propose to represent the RF signals from the explored tissues with a second order complex AR model [8]. Order 2 is the minimum order which enables the modeling of a bimodal signal, and it is consistent with our application, since the presence of USCA induces two peaks in the power spectrum density (PSD) of the signal. The position and amplitude of these peaks can be easily characterized by the *poles* of the AR model.

An AR model of order 2 is a parametric representation of a discrete signal $s(n)$ described as the output of a linear filter, driven by a white Gaussian noise $e(n)$ with zero mean and variance σ^2. The signal $s(n)$ is then given as

$$s(n) = e(n) - a_1 s(n-1) - a_2 s(n-2) \qquad (1)$$

where a_1, a_2 are the AR coefficients characterizing the signal. In the case of a complex signal, the AR parameters are complex. The PSD of the AR model of order 2 (which we call AR spectrum) can then be derived:

$$PSD_{AR2}(f) = \frac{\sigma^2}{|1 + a_1 e^{-j2\pi f} + a_2 e^{-j4\pi f}|^2} \qquad (2)$$

Such a spectrum corresponds to a bimodal distribution. The AR model may also be represented through the z-transform of the linear filter, which can equivalently be parameterized through its poles. These poles are derived from the estimated AR coefficients by simply solving a second order complex polynomial [8]. Let us denote the magnitude and phase of the complex poles as

$$p_1 = m_1 e^{j2\pi f_1} \, , \, p_2 = m_2 e^{j2\pi f_2} \qquad (3)$$

From the above development, the estimated positions of the peaks of the AR spectrum are given by f_1 and f_2, and the values (spectral magnitudes) of these peaks can be calculated by injecting f_1 or f_2 into equation 2.

For the discrimination of USCA from tissue, we propose to use the spectral magnitude of the second AR

spectral peak (SM_2). We illustrate the interest of this parameter on two synthetic signals: a fundamental frequency signal, simulating a signal issued from tissue; a harmonic frequency signal, simulating a signal issued from contrast agent, containing a fundamental and a second harmonic component.
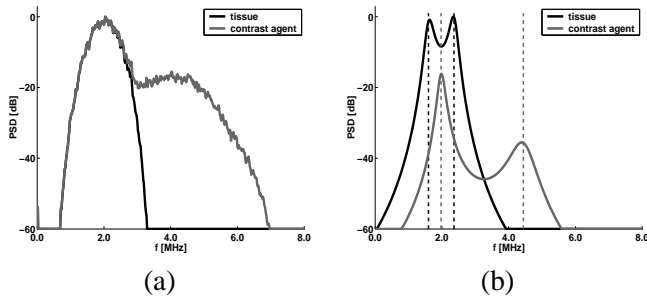

(a)   (b)

Figure 1: (a) PSD of the simulated signals, (b) corresponding AR spectrum, dashed lines indicate positions of the spectral peaks estimated from the poles

The PSD of the two signals, computed with the Fast Fourier Transform (FFT), can be seen in figure 1a, and the corresponding AR spectra, in figure 1b. Both for tissue and USCA the AR spectrum has two distinct peaks (or maxima), and when the PSD of the signal is bimodal (i.e. in the presence of USCA), these peaks coincide with the first and second harmonic components of the PSD. It can be observed that the second peak of the AR spectrum has a much lower amplitude in the case of a bimodal spectrum. This lower amplitude is related to two concurring effects: (1) both spectral peaks become lower as the distance between them increases; (2) the second spectral peak is lower, because the second harmonic component of a bimodal signal is lower than the fundamental one.

In the scope of the present work, the spectral AR estimation of order 2 is performed on the IQ signal (In-phase Quadrature [10]). The IQ image is partitioned into short windows along each acquisition line. We use overlapping windows of length corresponding roughly to the duration of the ultrasound pulse (around 1 mm). Estimation of the two first AR coefficients is then performed in each signal sample with the well known Burg method [8].

Due to the stochastic nature of the backscattered RF signal, short time spectral estimation results in a high variance of the estimated parameters. In order to improve the quality of the contrast agent detection, it is thus important to smooth these fluctuations while preserving discontinuities resulting from physical boundaries. In the scope of this work, we used a discontinuity adaptive smoothing technique that we initially developed for the purpose of autoregressive spectral estimation [7], [5].

Experimental methods and materials

The proposed detection method was evaluated on two kinds of data: (1) realistic simulations (2) in vitro acquisitions.

A composite tissue was first simulated, with three strips corresponding to tissue alone, tissue perfused with USCA at concentration (denoted χ) $1 \cdot 10^{-5}$, and tissue perfused with USCA at $\chi = 1 \cdot 10^{-4}$ (see figure 2a). RF simulated acquisitions were performed for different instrumental mechanical indexes (MI). Details on the simulation can be found in [11].

The experimental setup used for in vitro acquisitions is presented in fig. 2b. A phantom tissue (ATS Lab.) was immersed in a solution of physiological fluid (NaCl 0.9%). Sonovue^{TM} contrast agent, commercialized by Bracco, was subsequently added and the solution was homogenized with a magnetic stirrer. The echocardiographic probe PA230E (ESAOTE) of central frequency 2.5 MHz was used along with a MEGAS digital echographic scanner. A series of acquisitions was performed, with USCA concentration ranging from $2 \cdot 10^{-5}$ to $1 \cdot 10^{-4}$, and within a broad range of instrumental MI (from 0.10 to 0.36). It is to be noted
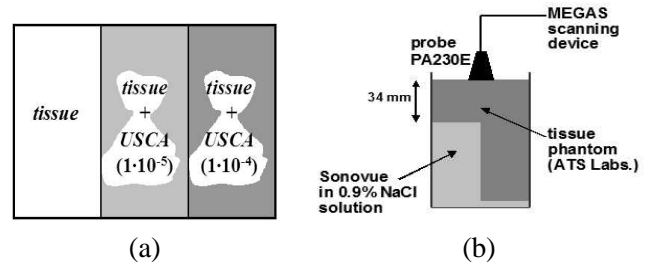

(a)   (b)

Figure 2: (a) scheme of the synthetic tissue used for simulations, (b) the setup for in vitro acquisitions

that the ultrasound probe was operating in the fundamental acquisition mode, and no special settings were made to enhance the harmonic component of the signal. This means that a part of the second harmonic component was truncated. To the contrary, the numerical probe used to obtain simulated data had a wide spectral band, therefore allowing acquisition of the full second harmonic component.

Results

Fig. 3 shows the results of processing two simulated RF images, obtained for two different values of MI (MI=0.10 in upper row, MI=0.36 in lower row). The envelope image, the field of the parameter SM_2 and the result of high-pass filtering (harmonic imaging, considered as reference) are shown. Whereas it is obvious that the envelope image cannot be used to discriminate between USCA-perfused and non-perfused areas, the parameter SM_2 enables to clearly differen-

tiate tissue alone and USCA-perfused tissue. The intensity of SM_2 is almost the same in both areas corresponding to perfused tissue with different USCA concentrations. The reference method, harmonic imaging, also performs very well in these images. However, contrarily to SM_2, the intensity of the high-pass filtered signal depends on the concentration of USCA. The relative stability of SM_2 with concentration is a characteristic desirable in the context of USCA detection. A

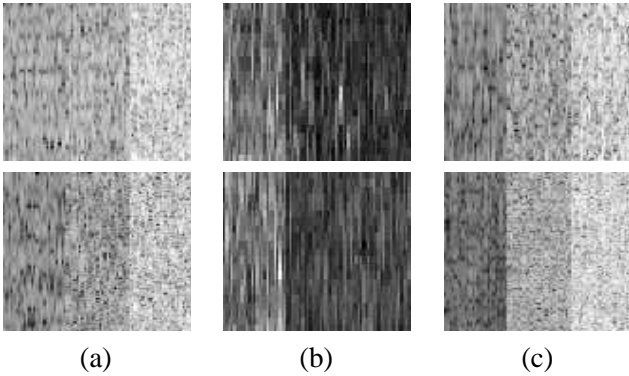| | | |
| (a) | (b) | (c) |

Figure 3: Results of processing simulated RF images: (a) envelope image, (b) detection parameter SM_2, (c) reference second harmonic image, for two different MI (see text)

plot showing the evolution of SM_2 in tissue perfused with USCA at different concentrations (MI=0.21) is presented in figure 4. SM_2 initially decreases for increasing concentrations, takes a minimum value which corresponds to the best detection of USCA, and then increases for higher values of concentration. Indeed, for very low concentrations the AR spectrum is the one of the tissue, and the two spectral peaks are symmetric about the central frequency. As concentration increases, the second harmonic component due to the USCA appears in the spectrum. Consequently, the second peak of the AR spectrum moves away from the first one and decreases. After a certain concentration is reached, the position of the second AR peak stabilizes. When concentration still increases, the second harmonic component gains more power and as a result, the second spectral peak increases again. However, it can be observed that within the available range of concentrations, SM_2 is relatively stable.

We subsequently processed 30 series of in vitro images corresponding to all the different couples *(χ, MI)* used during the experiment. Visual results are presented in two example frames extracted from the entire data set. The displayed frames have been chosen so that they correspond to representative cases in terms of USCA detection and result quality: $\chi = 5 \cdot 10^{-5}, MI = 0.36$: high concentration and high MI resulting in a strong signal from USCA (upper row in fig. 5) ; $\chi = 2 \cdot$
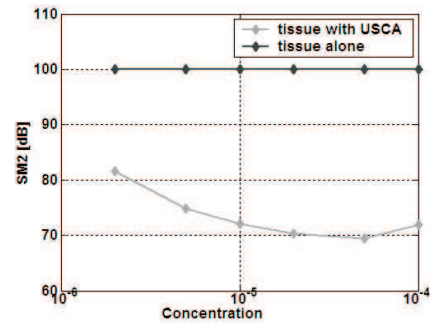

Figure 4: Plot showing the value of SM_2 averaged in regions corresponding to different concentrations of the USCA

$10^{-6}, MI = 0.10$: low concentration and MI, resulting in a weak signal from the USCA (lower row in fig. 5).

The variations of brightness of the USCA area in the envelope images (fig. 5b) reflect the differences of signal power discussed above. Fig. 5b presents the detection parameter SM_2 expressed in dB. The visual quality of these images is correct, and it illustrates the range of results obtained for different experimental conditions. The contrast agent can be clearly seen as a dark area surrounded by the bright region of the phantom. The spectral magnitude of the second peak is higher in the phantom tissue, and lower in the contrast agent, which is consistent with the framework presented in the methodological section and with simulation results. It can be
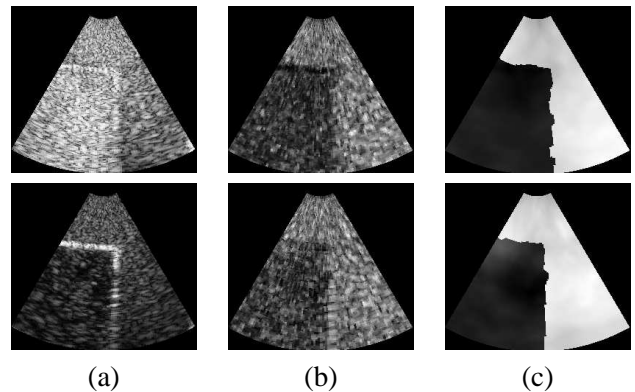

| | | |
| (a) | (b) | (c) |

Figure 5: Results of processing in vitro data: (a) envelope image, (b) detection parameter SM_2, (c) SM_2 processed with discontinuity-adaptive smoothing, for two different acquisition conditions (see text)

clearly seen on the images that the variance of the SM_2 estimator is relatively high. In order to reduce it and to obtain a binary map of perfused areas, we apply a discontinuity adaptive (DA) smoothing algorithm [7]. Fig. 5c shows results of smoothed detection provided by the algorithm. One can see that the USCA appears as a homogeneous, dark area, and the detected borders cor-

respond well to the real boundaries of the phantom. DA smoothing gave similar results on all series from this data set of in vitro acquisitions. Due to the stability of the detection parameter with concentration and MI, the same values of the algorithm hyperparameters (defining the threshold level and the importance of the smoothness constraint) were used for the entire sequence.

Discussion

Experiments on simulated RF images showed that the method enables to discriminate between tissue and tissue perfused with USCA, over a wide range of concentrations and instrumental MI. A relative stability of the method was observed with respect to these parameters, and results from in vitro experimental data confirmed the observations. This indicates that the technique we propose can be used as a robust detector, adapted for the segmentation of USCA-perfused regions. The SM_2 detector is particularly attractive, since it allows detection of USCA in difficult conditions, at low concentration and low MI.

A possible drawback of our method is a relatively high variance of the estimator. However, this drawback is largely compensated by the stability of the SM_2 estimator to experimental conditions. This stability makes it suitable for segmentation with the DA smoothing algorithm. Indeed, the detection of the USCA-perfused area is almost perfect, not only in the two example images, but also in the entire data set. It is worth noting that such a result could not be obtained on high pass-filtered images, since their contrast and overall aspect varies dramatically with concentration and instrumental MI, requiring fine tuning the hyperparameters to each image.

Conclusion

A common drawback of current contrast imaging techniques is that they are USCA-, MI- and concentration-dependent. The proposed method has the advantage of being relatively stable against acquisition conditions, in particular concentration of the USCA, and to operate on a single image. It can be used as a robust contrast agent detector, and is suitable as the basis for segmentation of USCA perfused regions of the muscle.

In perspective, the proposed approach need to be validated on in vivo cardiac images, as well as on other types of ultrasound contrast agents, in order to evaluate its sensitivity and accuracy when used in clinical conditions.

Acknowledgement

References

[1] M. Arditi, T. Bernier, and M. Schneider. Preliminary study in differential contrast echography. *Ultrasound in Medicine and Biology*, 23(8):1185–1194, 1997.

[2] J. Borsborn, C. T. Chin, and N. d. Jong. Experimental validation of a nonlinear coded excitation method for contrast agent. In *IEEE UFFC Symposium*, 2002.

[3] A. Bouakaz, B. Krenning, W. Vletter, F. T. Cate, and N. d. Jong. Imaging contrast agent and tissue at higher harmonics. In *IEEE UFFC Symposium*, 2002.

[4] N. d. Jong, A. Bouakaz, and F. J. T. Cate. Contrast harmonic imaging. *Ultrasonics*, 2002.

[5] I. Dydenko, D. Friboulet, J.-M. Gorce, J. D'hooge, B.Bijnens, and I. E. Magnin. Towards ultrasound cardiac image segmentation based on the radiofrequency signal. *Med Image Ana*, to be published, 2003.

[6] F. Forsberg, W. T. Shi, and B. B. Goldberg. Subharmonic imaging of contrast agents. *Ultrasonics*, 38:93–98, 2000.

[7] J.-M. Gorce, D. Friboulet, I. Dydenko, J. D'hooge, B. H. Bijnens, and I. E. Magnin. Processing radio frequency ultrasound images: A robust method for local spectral features estimation by a spatially constrained parametric approach. *IEEE Trans UFFC*, 49(12):1704–1719, 2002.

[8] S. M. Kay. *Modern Spectral Estimation : theory and application*. Alan V. Oppenheim, signal processing series Prentice Hall, 1988.

[9] K. Morgan, M. Averkiou, and K. Ferrara. The effect of the phase of transmission on contrast agent echoes. *IEEE Trans UFFC*, 45(4):872–875, 1998.

[10] J. G. Proakis and D. G. Mankolakis. *Digital signal processing: principles, algorithms and applications*. Prentice Hall International, 1996.

[11] N. G. Rognin. *Imagerie de contraste en echographie medicale, 196/2002*. PhD thesis, Universite Claude Bernard Lyon 1, 2002.

[12] D. H. Simpson, C. T. Chin, and P. N. Burns. Pulse inversion doppler: a new method for detecting nonlinear echoes from microbubble contrast agent. *IEEE Trans UFFC*, 46(2):372–382, 1999.